

- 31 Arbas, E. A. and Calabrese, R. L. (1987) *J. Neurosci.* 7, 3945–3952
- 32 Simon, T. W., Opdyke, C. A. and Calabrese, R. L. (1992) *J. Neurosci.* 12, 525–537
- 33 Evans, B. D. and Calabrese, R. L. (1991) *Peptides* 12, 897–908
- 34 De Schutter, E. (1989) *Comput. Biol. Med.* 19, 71–81
- 35 De Schutter, E., Angstadt, J. D. and Calabrese, R. L. *J. Neurophysiol.* (in press)
- 36 Hodgkin, A. L. and Huxley, A. F. (1952) *J. Physiol.* 117, 500–544
- 37 Wang, X.-J. and Rinzler, J. (1992) *J. Neural Comp.* 4, 84–97
- 38 Wang, X.-J., Rinzler, J. and Rogawski, M. A. (1992) *J. Neurophysiol.* 66, 839–850
- 39 Tierney, A. J. and Harris-Warrick, R. M. (1992) *J. Neurophysiol.* 67, 599–609

## The cerebellum and VOR/OKR learning models

Mitsuo Kawato and Hiroaki Gomi

*Although one particular model of the cerebellum, as proposed by Marr and Albus, provides a formal framework for understanding how heterosynaptic plasticity of Purkinje cells might be used for motor learning, the physiological details remain largely an enigma. Developments in computational neuroscience and artificial neural networks applied to real control problems are essential to understand fully how workspace errors associated with movement performances can be converted into motor-command errors, and how these errors can then be used as one kind of synaptic input by motor-learning algorithms that are based on biologically plausible rules involving heterosynaptic plasticity. These developments, as well as recent advances in the study of cellular mechanisms of synaptic plasticity, form the basis for the detailed computational models of cerebellar motor learning that have been proposed. These models provide hints toward resolving a long-standing controversy in the oculomotor literature regarding the sites of adaptive changes in the vestibulo-ocular reflex (VOR) and the optokinetic eye movement response (OKR), and suggest new experiments to elucidate general mechanisms of sensory motor learning.*

The problem of controlling goal-directed limb movements can be partitioned conceptually into a set of information-processing subprocesses; trajectory planning, coordinate transformation from extracorporal space to intrinsic body coordinates and motor command generation. These subprocesses are required to translate the spatial characteristics of the target or goal of the movement into an appropriate pattern of muscle activations<sup>1,2</sup>. However, fast, smooth and coordinated movements cannot be realized by just feedback control alone because, in biological motor control systems, the delays associated with feedback loops are long and the feedback gains are low. Thus, internal predictive models of the motor apparatus need to be utilized in the course of these computations<sup>3</sup>. The internal models in the brain must be acquired through motor learning in order to accommodate the changes that occur with the growth of controlled objects such as hands, legs and torso, as well as with the unpredictable variability of the external world.

Where in the brain are internal models of the motor apparatus likely to be stored? First, the locus should exhibit a remarkable adaptive capability, which is essential for acquisition and continuous update of internal models of the motor apparatus. A number of physiological studies<sup>4,5</sup> have suggested that the cer-

ebellum may play important functional roles in motor learning, and demonstrated remarkable synaptic plasticity in the cerebellar cortex. Second, biological objects of motor control by the brain, such as arms, speech articulators and the torso, possess many degrees of freedom and complicated nonlinear dynamics. Correspondingly, the neural internal models should receive a broad range of sensory inputs and possess a capacity high enough to approximate complex dynamics. Extensive sensory signals carried by mossy fiber inputs and an enormous number of granule cells in the cerebellar cortex seem to fulfill the above prerequisites for internal models. Finally, the cerebellar symptoms usually known as the 'triad' of hypotonia, hypermetria and intention tremor<sup>6</sup> could be understood as a degraded performance when motor control is forced to rely solely on negative feedback after the internal models are destroyed, cannot be updated, or both. Precise, fast and coordinated movements can be executed if accurate internal models of the motor apparatus can be used during trajectory planning, coordinate transformation and motor control; a pure feedback control, involving long feedback delays and small gains, can attain only a poor performance in these computations and usually leads to oscillatory instability for forced fast movements. It is clear that internal models are essential for normal motor coordination; the question that must now be asked is how might these internal models be acquired in the cerebellum through motor learning?

### Supervised motor learning of internal models

Controlled objects in biological movement can generally be described as multi-variable nonlinear dynamic systems whose inputs are muscle tensions, joint torques or firing rates of the nerve fibers that innervate muscles, and whose outputs are muscle lengths, joint angles or the position of the hand, for example, in Cartesian coordinates. Thus, the direction of information flow in the controlled objects is from the motor commands to the movement trajectory. Following robotics jargon, we state that this direction of the information flow is forward, and the opposite direction, inverse. Accordingly, internal models of the motor system can be divided into two types: forward models and inverse models. By 'forward model' we mean a neural representation of the transformation from motor commands to the resultant behavior of the controlled object. In other words, a forward model is just a simple model of the controlled object, and can be used as its substitute. If the actual motor command given to the motor

*Mitsuo Kawato and Hiroaki Gomi are at the ATR Human Information Processing Research Laboratories, Kyoto 619-02, Japan; Mitsuo Kawato is also associated with the Laboratory of Parallel Distributed Processing, Research Institute for Electronic Science, Hokkaido University, Sapporo, Hokkaido 060, Japan.*

apparatus is also fed as an input to the forward model, the output of this model will predict the realized trajectory. The neural computation time for this prediction (say 30 ms) is expected to be much shorter

than the external visual or proprioceptive feedback delay (say from 100 to 200 ms). Thus, if a forward model is used in the internal feedback loop (Fig. 1A), feedback control performance is improved significantly since large external feedback delays can be avoided<sup>7</sup>. On the other hand, more sophisticated feedforward control can be achieved through an inverse model of the controlled object<sup>8-10</sup>. By 'inverse model' we mean a neural representation of the transformation from the desired movement of the controlled object to the motor commands required to attain these movement goals. Because the inverse model possesses input-output transfer characteristics that are the inverse of those of the controlled object, the cascade of the two systems gives an approximate identity function (Fig. 1B). That is, if a desired trajectory is given to the cascade the realized trajectory is fairly close to the desired trajectory. Thus, accurate inverse models could be used as ideal feedforward controllers. Training of inverse models is therefore crucial to the performance in feedforward control.

How can an internal inverse model be acquired<sup>11</sup>? If a computational 'teacher' can provide the correct motor commands, motor learning can be done in the framework of what is known as the Widrow-Hoff rule<sup>12,13</sup>, consistent with biologically demonstrable heterosynaptic plasticity processes (Fig. 1C; and see Box 1). In the context of motor learning, however, it is unrealistic to assume the existence of a teacher with access to the correct motor commands prior to the learning of the movement pattern itself. Rather, it is more realistic to assume that a teacher has access only to the movement trajectory desired for the controlled object. For example, parents teach their children the correct pronunciation of words by providing speech samples in acoustic space, but cannot directly communicate the neuronal firing patterns that activate articulator muscles. Correspondingly, a biologically plausible teacher for a neural network would not have direct access to the correct pattern of articulatory commands, but instead would only have access to the desired 'higher level' trajectory and the resultant discrepancies or errors between the desired and currently produced trajectories. In order to train the inverse model, such trajectory errors must first be converted to motor command coordinates.

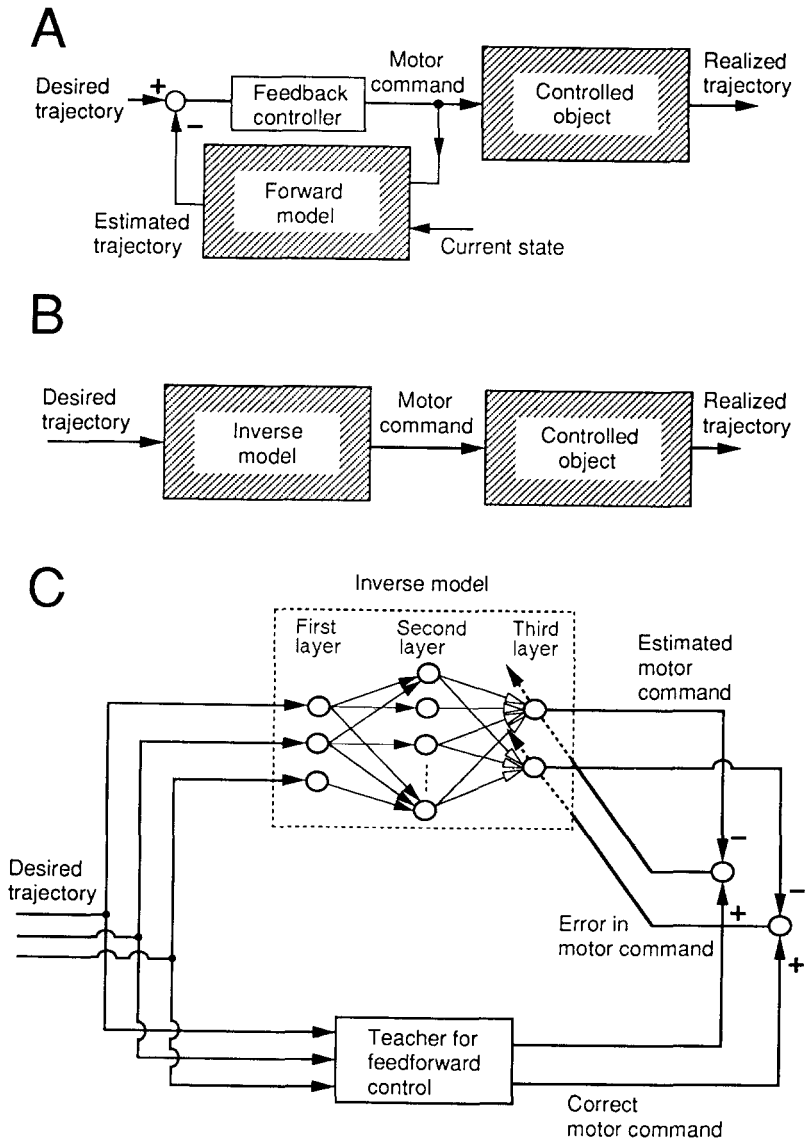


**Fig. 1.** Forward (A) and inverse (B) neural models of the controlled object. The engineering jargon 'controlled object' here means a concrete physical thing which should be controlled by the CNS. Examples are industrial robotic manipulators, airplanes, hands, legs and the torso. (C) The simplest learning scheme for acquiring the inverse model when a perfect teacher exists. In these figures, circles represent neurons and arrows represent synapses. In (C) the efficacies of synapses shown by open arrows change in proportion to the product of the synaptic input from the second layer and the error signal shown by the broken line (see Box 1 for this Widrow-Hoff rule). The inverse model box represents a connectionist feedforward network without feedback connections from the higher layer to the lower layer, or without connections within any one layer. It could be extended to more general networks with these feedback connections as models of cortical layers. As the controlled object, we have in mind a single joint articulated by agonist and antagonist muscles. The three neurons in the first layer of the inverse model box represent the desired joint angle, the desired joint angular velocity and the desired joint angular acceleration as functions of time, respectively. The two output neurons in the third layer represent muscle activation levels for the agonist and antagonist pair. Both forward and inverse models can be considered to be the cascades of transformations between motor command (e.g. joint torques, muscle activations) and linkage motion (e.g. joint angular position, velocity, acceleration) coordinates, and between linkage motion and controlled object motion (e.g. spatial position, velocity and acceleration of the hand) coordinates. Such transformations represent, respectively, system dynamics and kinematics.

#### Box 1. Associative LTP and LTD and the Widrow-Hoff rule

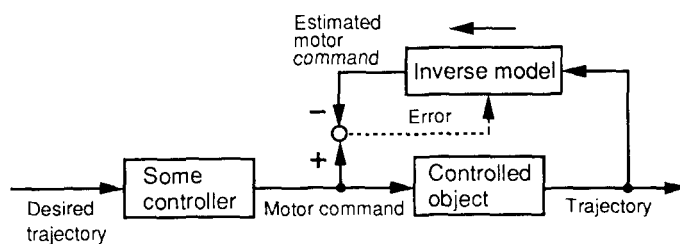
Associative long-term potentiation (LTP) and long-term depression (LTD) could be formulated as follows: the rate of change of the synaptic efficacy of a type 1 synapse (classical synapse, shown by open arrows in Fig. 1C) is proportional to the product of the inputs to the type 1 and type 2 (modulator synapse, shown by filled arrows with broken lines in Fig. 1C) synapses. In the Widrow-Hoff rule, the rate of change of the efficacy of a type 1 synapse is proportional to the product of the type 1 input and the error signal (the difference between the teaching signal and the actual output of the neuron). Thus, the Widrow-Hoff rule could be implemented by the associative LTP or LTD if the type 2 synaptic input represents the error signal.

Three learning schemes have been proposed to address the error conversion issue. In the direct inverse modeling approach (Fig. 2A), the inverse model receives the realized trajectory as an input, and outputs an estimated motor command. The difference between the estimated motor command and the actual motor command is used as the error signal for training the inverse model<sup>8,14</sup>. Although this learning scheme is simple, it has several drawbacks. For example, the inverse model cannot be used for control during training because in this case it is the desired trajectory rather than the realized trajectory that needs to be used as the input to the inverse model. Furthermore, there is no mathematical guarantee that a desired trajectory is rigorously realized after learning. Another major problem with this approach is that it cannot properly control a redundant object (i.e. a controlled object whose degrees of freedom of motor commands exceed the degrees of freedom of the state variables, such as a primate limb). Because many sets of motor commands correspond to a single movement for redundant objects, a unique, invertible relationship between the desired goal and the motor command cannot exist. Thus, this learning scheme usually generates a faulty motor command, as pointed out by Jordan<sup>15</sup>. A simple example of a kinematically redundant controlled object (i.e. the degrees of freedom of the mechanical linkage exceed the degrees of freedom of the task space) is a three-joint arm within a plane, for which the three joint angles (three degrees of freedom) cannot be uniquely determined even when the hand position is given in Cartesian coordinates (two degrees of freedom). A simple example of a dynamically redundant controlled object (i.e. the number of actuators exceeds the degrees of freedom of the mechanical linkage) is a single joint with a pair of muscles, for which the agonist and antagonist muscle tensions (two degrees of freedom) cannot be uniquely determined even when the joint-angle timecourse (single degree of freedom) is specified.

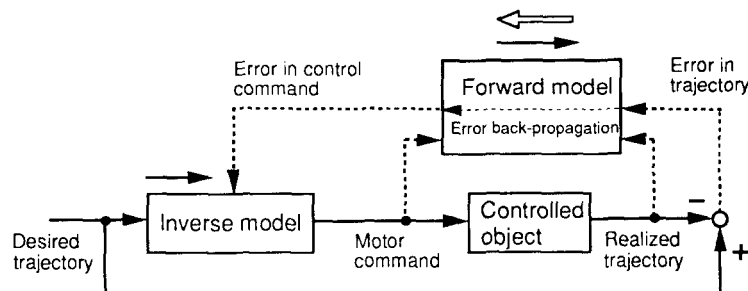
In the forward-inverse modeling approach (see Fig. 2B)<sup>15,16</sup>, the forward model of the controlled object is first learned by monitoring both the input and the output of the controlled object. Then, the desired movement trajectory is fed to the inverse model to calculate the feedforward motor command. The resulting error in the trajectory space is back-propagated<sup>17</sup> through the forward model to calculate the error in the motor command space (see Box 2), which is then used as the error signal for training the inverse model. This approach resolves several shortcomings inherent to the direct inverse method; learning and motor control can be done simultaneously, the goal-directed properties of learning are guaranteed and the scheme can be applied to redundant controlled objects<sup>15</sup>. Backpropagation itself, however, is difficult to implement neuronally<sup>18</sup> since we do not know the fast retrograde physiological mechanisms that carry information along the axons. It is possible to avoid backpropagation in the forward-inverse modeling approach, but the substitute processes are generally complicated.

In the feedback-error-learning approach (Fig. 2C), a summation of the feedback motor command and the feedforward command generated by the inverse model is fed to the controlled object, and the feedback

## A Direct inverse modeling



## B Forward and inverse modeling



## C Feedback error learning

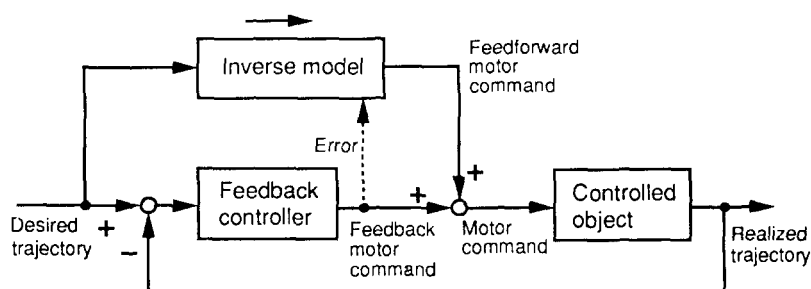
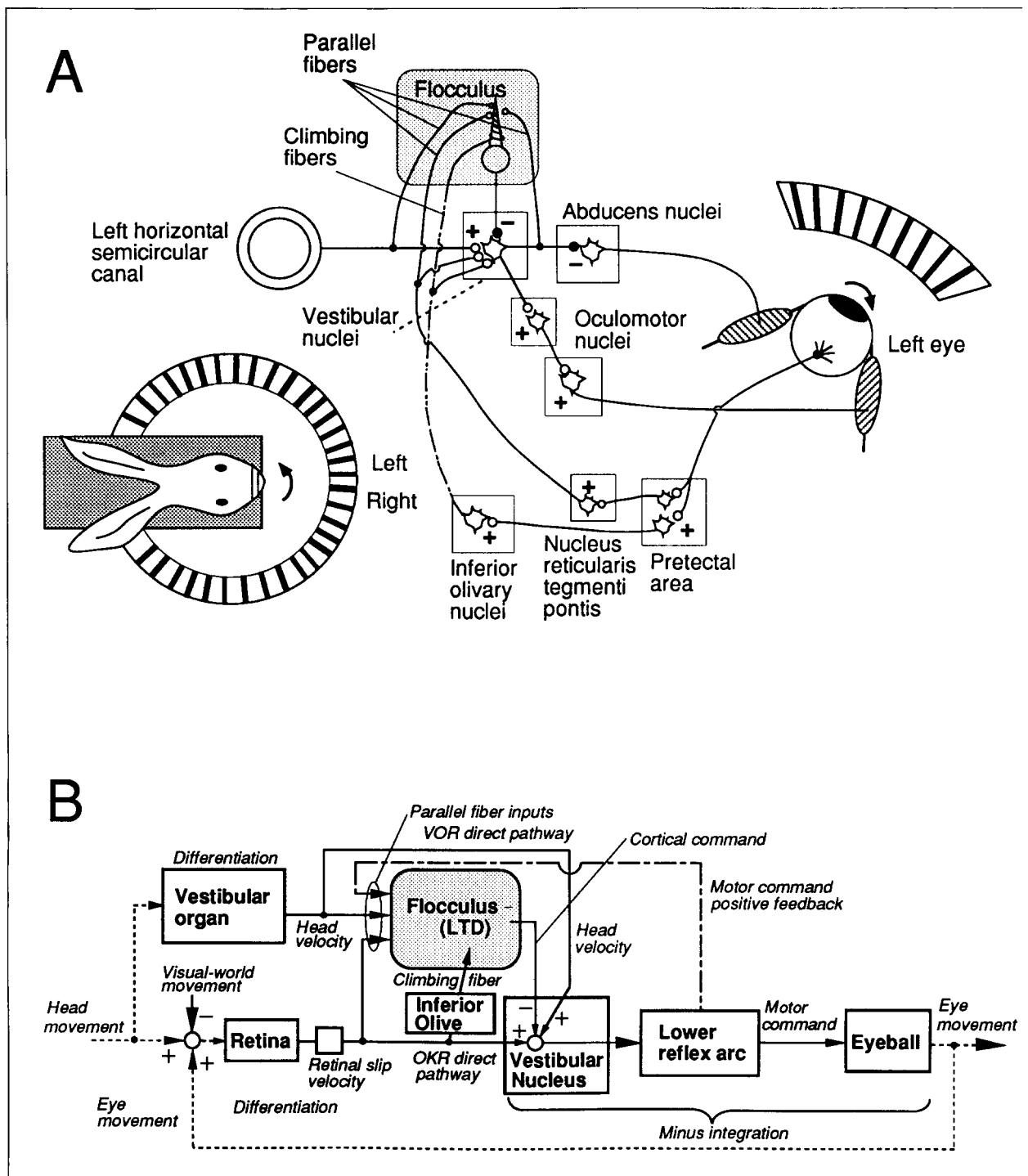


**Fig. 2.** Three computational schemes for acquiring an inverse model through learning. (A) Direct inverse modeling approach. (B) Forward and inverse modeling approach. (C) Feedback-error-learning approach. The direction of information flow is indicated by solid lines. Broken lines show information used for training. Filled arrows attached to forward and inverse models show their information-processing directions. The open arrow in (B) represents the information-flow direction in the backpropagation calculation. Refer to the text for more detailed descriptions.

### Box 2. Backpropagation through forward model

For simplicity, let us suppose that a three-layer feedforward network, such as that shown in the dashed rectangle of Fig. 1C provides a kinematic forward model of a kinematically redundant arm. That is, the three neurons in the first layer represent the three joint angles of the arm, and the two in the third layer represent Cartesian coordinates of the hand position. The visual system can measure the positional error between the hand and the desired location in Cartesian coordinates. This positional error, calculated for each output neuron, is multiplied by the individual synaptic weight from the second layer to the third layer, and then is assigned to that synapse. For each neuron in the second layer, all the above weighted errors are summed to give the error for that neuron. Exactly the same procedure is repeated between the first layer and the second layer. Then, for each neuron in the first layer, the error in the joint space can be calculated.



controller transforms the trajectory error into the motor command error<sup>9</sup>. The inverse model is trained during motor control using the feedback motor command as the error signal. In this scheme, the feedback controller plays the role of a linear approximation of the inverse model of the controlled object, and converts the trajectory error into the motor command error. The feedforward controller does not mimic the feedback controller, but acquires the fully nonlinear inverse model by trying to reduce the feedback motor command.

This approach was applied to the learning control of robots possessing kinematic or dynamic redundancy and a 300 ms feedback loop delay<sup>19,20</sup>. Because of the feedback delay, the realized trajectory was compared with the desired trajectory some time earlier in the feedback controller. Although this seems quite diffi-

cult, this feedback error learning process was successful in these situations.

### Adaptive models of VOR/OKR

Cerebellar motor learning has been most intensively studied in the vestibulocerebellum using the vestibulo-ocular reflex (VOR). When the head is turned, the VOR normally acts to stabilize retinal images by generating smooth eye movements that are equal and opposite to the rotary head movements. Under experimental manipulations of retinal slips using magnifying spectacles, inversion prisms or by rotating a visual screen, the gain of the VOR (the ratio of eye to head movement) changes. Such VOR adaptation is abolished when the flocculus is destroyed in cats, rabbits and monkeys, or when only the visual climbing-fiber pathway is destroyed in

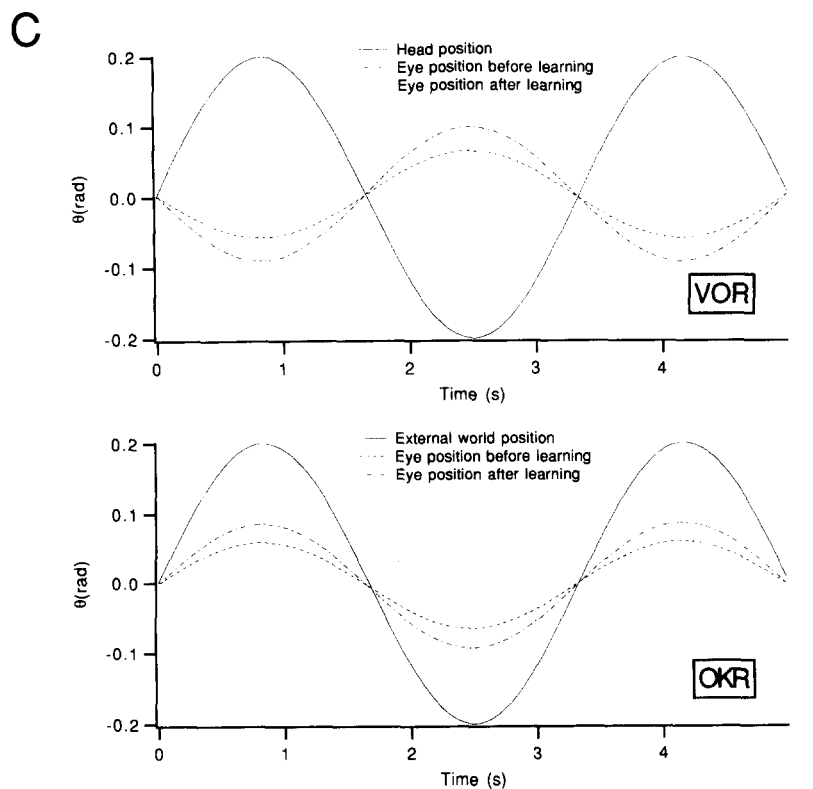


**Fig. 3.** A neural circuit diagram and a block diagram for horizontal VOR and OKR, and simulation results. (A) A schematic diagram of neural circuit for horizontal VOR and OKR. (B) A block diagram of adaptive modification of VOR and OKR by the flocculus. Information flow via the external world is shown by broken lines. Neural pathways are shown by solid lines. The motor command positive feedback pathway is shown by a chain line because origins in the brain stem are not clear. (C) Simulation results for adaptive modification of VOR and OKR. The model neural network was constructed as shown in (B) while assuming a 10 ms delay for the motor command feedback to the flocculus, and a 20 ms delay for the retinal slip feedback. System performance during head rotation in the dark (VOR, upper panel) and during visual screen rotation (OKR, lower panel) is compared between before learning (broken curve) and after training (chained curve). Oscillation of 0.3 Hz and 0.4 radian peak-to-peak was used both for VOR and for OKR. During 1000 s of training sessions shown in (A) the visual screen was rotated sinusoidally at 0.2 Hz and 0.4 radians peak-to-peak. The head was rotated by a stochastic process with a similar timecourse and amplitude. Parameters of visual and vestibular stimuli close to those of rabbit experiments<sup>35,36</sup> were chosen. The VOR gain increased from 0.29 to 0.45 while the OKR gain increased from 0.29 to 0.43 after 1000 s training. Gain changes of 0.1 to 0.15 within one hour are usually observed in rabbits.

rabbits (see Ref. 21 for a review). The site of motor learning in primates is still in dispute and will be discussed later. Here we review the model for rabbits.

Marr<sup>22</sup> and Albus<sup>23</sup> proposed a detailed model of the cerebellum that can form associative memories between particular patterns on parallel fiber inputs and Purkinje cell outputs. The basic idea was that the synapses between the parallel fibers and Purkinje cells could be modified by inputs from the climbing fibers. The presence of the putative heterosynaptic plasticity of Purkinje cells was demonstrated as long-term depression (LTD)<sup>24</sup> (see Box 3). Although previous studies failed to detect plastic changes, several laboratories recently confirmed the LTD while using different preparations<sup>25-28</sup>. Fujita<sup>29</sup> expanded the basic Marr-Albus model to incorporate

dynamic responses, and proposed that the cerebellum is an adaptive filter that can learn to compensate for the dynamical characteristics of the oculomotor plant. He simulated adaptive modification of the VOR based on both LTD and the hypothesis, proposed by Ito<sup>7,21,24</sup>, that the synapses between parallel fibers and Purkinje cells of the cerebellar flocculus are the site of modification. Climbing fiber activities are assumed to reflect motor performance error information conveyed by retinal slip velocity<sup>30,31</sup> (see Box 3).

Horizontal VOR is regulated by a three-neuron reflex arc as well as by the microzone<sup>32</sup> of the flocculus called the H-zone<sup>33</sup>, which also participates in the control of the optokinetic eye movement response (OKR)<sup>21</sup>. The OKR moves the eye in the same direction as the visual field motion to stabilize the retinal image, and shares major neural mechanisms with the VOR. In the VOR the vestibular signal is used in feedforward control, while in the OKR the visual signal is used in feedback control. A schematic diagram of the neural circuitry for the VOR and OKR is shown in Fig. 3A. There it can be seen that when the head is rotated leftward, the semicircular canal sends the head rotational velocity to the vestibular nucleus and to the flocculus, and the eye is rotated rightward. If the VOR is not perfect, images move on the retina, and the retinal slip information is sent back both to the vestibular nucleus and to the flocculus by the climbing fibers and the mossy fibers. This retinal slip information is the sensory input used in the OKR. Additionally, examination of eye velocity components in simple spikes of Purkinje cells revealed that the corollary dis-

charge of the motor command forms a positive feedback loop through the Purkinje cells and the vestibular nucleus<sup>34,35</sup>. Thus, the Purkinje cells of the flocculus receive three kinds of synaptic inputs via parallel fibers: the head velocity signal measured by the vestibular organ, the retinal slip signal measured by motion detectors in the retina and sent from the nucleus reticularis tegmenti pontis, and the eye velocity signal. The retinal slip velocity, conveyed by the climbing fibers to the Purkinje cells, is the error signal in the LTD, and is essential for adaptation of the OKR as well as the VOR (Ref. 36).

Details of our neural network model are shown in schematic form in Fig. 3B, where it can be seen that if the external world is stationary, the retinal slip is the summation of the head and eyeball velocities. The eyeball velocity required to stabilize the retinal image

### Box 3. LTD of Purkinje cells

Associative LTD found in Purkinje cells could be modeled using the following heterosynaptic plasticity rule: the rate of change of the synaptic efficacy of a single parallel fiber synapse is proportional to the negative product of the firing rate of that synapse input and the increment of the climbing fiber firing rate from its spontaneous level<sup>a</sup>. This single rule reproduces both LTD and LTP found in Purkinje cells. When the climbing fiber and the parallel fiber are simultaneously stimulated, the synaptic efficacy of the parallel fiber decreases. In contrast, the parallel fiber synaptic efficacy increases when only the parallel fiber is stimulated (the climbing fiber firing frequency is lower than its spontaneous level). Thus, the Widrow–Hoff rule can be implemented for LTD in Purkinje cells if the climbing fiber input represents the error signal. The sign conversion should be noted because Purkinje cells are inhibitory neurons.

#### Reference

a Fujita, M. (1982) *Biol. Cybern.* 45, 195–206

is then equal and opposite the head velocity. The time derivative of the error between the desired and realized eye velocity is sent to the vestibular nuclei and to the flocculus via the visual climbing-fiber and the OKR feedback pathways. Thus, the OKR closed loop constitutes a negative, derivative-type feedback controller, whose activity is monitored by the climbing fibers as the error signal, and the VOR constitutes purely a feedforward control. Consequently, the adaptive function of the flocculus can be understood on the basis of our feedback-error-learning scheme (see Fig. 2C). In this scheme, the cerebellar flocculus in combination with the basic three-neuron VOR arc can be interpreted as a neural network that can acquire the inverse dynamics model of the oculomotor plant. In a closer comparison of Fig. 3B and Fig. 2C, head movement, eye movement, the retina, retinal slip velocity, the flocculus, climbing fibers and the eye ball in Fig. 3B correspond to desired trajectory, realized trajectory, feedback controller, feedback motor command, inverse model, error and controlled object in Fig. 2C, respectively. The dashed part of the OKR negative feedback loop in Fig. 3B is physical rather than neural. We note that feedback loops always contain some physical part, irrespective of sensory modality. The essential characteristic of feedback error learning in the VOR/OKR adaptation system is that the error signal for training the feedforward controller is generated by a negative feedback controller.

We simulated a simultaneous adaptation of the VOR/OKR based on the model illustrated in Fig. 3B to examine whether the quantitative results from rabbit experiments can be reproduced<sup>37</sup>. The vestibular input to the flocculus was assumed to code the head velocity signal as an analog firing rate. The visual input to the flocculus was assumed to code the retinal-slip velocity. The eye velocity signal to the flocculus was assumed to code the motor command calculated by the flocculus. The firing rate of the climbing fibers was assumed to represent a linear combination of the retinal-slip position, velocity and acceleration, but experimental data showed that the velocity term was dominant<sup>31</sup>, and thus simulated. Both the turntable on

which the animal was fixed and the drum on which visual stimuli were presented were independently rotated during a training period of 1000 s (Fig. 3A) according to the experimental paradigm used by Ito and Nagao<sup>21</sup>, and their colleagues. The dynamics of the eyeball were modeled by taking into account its mass, viscosity and stiffness. Three kinds of parallel-fiber synaptic efficacy changes were simulated, based on the LTD rule illustrated in Box 3, while taking an ensemble average of many Purkinje cells in the flocculus. The VOR and OKR gains increased as shown in Fig. 3C, due to increases in the synaptic efficacies of all three kinds of parallel fiber inputs<sup>37</sup>. The magnitudes and timecourses of the gain changes were comparable to the rabbit experimental data<sup>21</sup>.

### Computational constraints on the site of adaptive changes

There has been a long-standing controversy about the site of the adaptive change of the VOR in primates. Lisberger and Miles<sup>38</sup> proposed that the sites of modification are the vestibular-input synapses of flocculus target neurons (FTN) in the vestibular nuclei receiving monosynaptic inhibition from the flocculus (known as the FTN hypothesis). In contrast, Watanabe<sup>39</sup> concluded that the site in monkeys, just as in rabbits, is the flocculus. Anatomical and physiological clues, which may resolve this controversy, have been recently obtained. Gerrits and Voogd<sup>40</sup> demonstrated that the rostral half of the traditionally defined monkey flocculus, from which the first group of authors mainly recorded<sup>34</sup>, was homologous to the ventral paraflocculus, but not to the flocculus in the rabbit. Then, Nagao<sup>41</sup> found that activities of Purkinje cells in the ventral paraflocculus and the flocculus *per se* are different during VOR, smooth pursuit eye movement and VOR suppression. The ventral paraflocculus results are in agreement with reports of Miles and Lisberger, while the flocculus results are in agreement with reports by Watanabe. These new findings seem to favor the site of adaptive change of the VOR being localized to the flocculus for primates.

Results from recent computational studies may also be used to address the issue of the adaptation site in primates. Sejnowski and Lisberger<sup>42</sup> developed a dynamical neural network model of the VOR and smooth pursuit eye movement. A recurrent back-propagation algorithm was used simply as an optimization procedure, not as a biological learning model, to determine how the network would reduce the amplitude of the VOR while maintaining accurate pursuit. Reductions of VOR gain were achieved by decreasing the connection weights in the vestibular input to the FTN. The connection weights in the vestibular input to the flocculus first increased and then decreased. The authors interpreted these results as supporting the flocculus hypothesis. In the context of the three schemes of supervised motor learning shown in Fig. 2, it is clear that both the vestibular inputs and the retinal slip signals must be available at the site of modification. On the one hand, the FTN hypothesis is most readily formulated as one version of feedback error learning. On the other hand, Lisberger<sup>38</sup> suggested that the flocculus provides error signal information to FTN neurons. However, as their own data and those from others show<sup>34,41</sup>, the activities of flocculus Purkinje cells reflect vestibular

input and eye movement, as well as retinal slip. Thus, it seems that if the FTN hypothesis is true, all three supervised learning schemes must be modified in order to accommodate the situations in which the error signal is carried by the flocculus output. It is quite probable that several different combinations of adaptive sites are involved in VOR learning. Computational constraints, however, demonstrate the difficulties in developing the model for all the possible sites that rely solely on local learning rules such as LTP or LTD, and on the required error signal in the appropriate coordinates.

### Models of sensory motor learning in the cerebellum

Several research groups have found that different regions of the cerebellum play important roles in the learning of different motor behaviors, such as arm movement, locomotion, posture control and classical conditioning of eye-blink responses (see for example Ref. 33 for a review). Although the input and output, and the functional roles of different regions of the cerebellum are vastly different, the neural circuit in the cerebellar cortex is rather uniform. Given this histological uniformity, several authors have extended the basic LTD-based oculo-motor reflex models in a search for a computational framework in which motor learning in different cerebellar regions is coherently understood.

Houk and Barto<sup>43</sup>, and colleagues proposed an adjustable pattern generator (APG) model of the cerebellum. Temporal patterns of movements are acquired through motor learning, based on the LTD of Purkinje cells in combination with positive feedback loops formed between cerebellar deep nuclei and brain-stem nuclei, such as the cerebellar reverberating circuit<sup>44</sup>. Artificial neural network models with recurrent connections that can learn and generate arm trajectories<sup>15,45</sup> were used, along with a learning scheme that is mathematically based on associative reward-penalty learning<sup>46</sup>. One of its attractive features is that, in their scheme, a motor pattern is selected and generated, which is impossible with a simple internal forward or inverse model. Correspondingly, however, learning is more difficult.

Miall *et al.*<sup>47</sup> proposed that the cerebellum forms two types of internal models. One model is a forward model of the motor apparatus like that in Fig. 1B. The second is a model of the transport time delays in the control loop (due to receptor and effector delays, axonal conductances and cognitive processing delays). The second model delays a copy of prediction made by the first model, so that it can be compared in temporal registration with actual sensory feedback from the movement. The second model resolves the difficulty of temporal mismatching between the sensory signal delayed by the feedback loop and the output calculated by internal models. In manual tracking of visual targets by humans and primates, the control performance became noisier and more unstable when an extra time delay was inserted before presenting the visual target. Several experimental phenomena like this were reproduced by their model.

We proposed a coherent model of cerebellar motor learning shown in Fig. 4, based on the feedback-error-learning scheme<sup>3,9,19,37,48</sup>. Premotor networks, the cerebellar cortex, climbing fiber inputs, and the

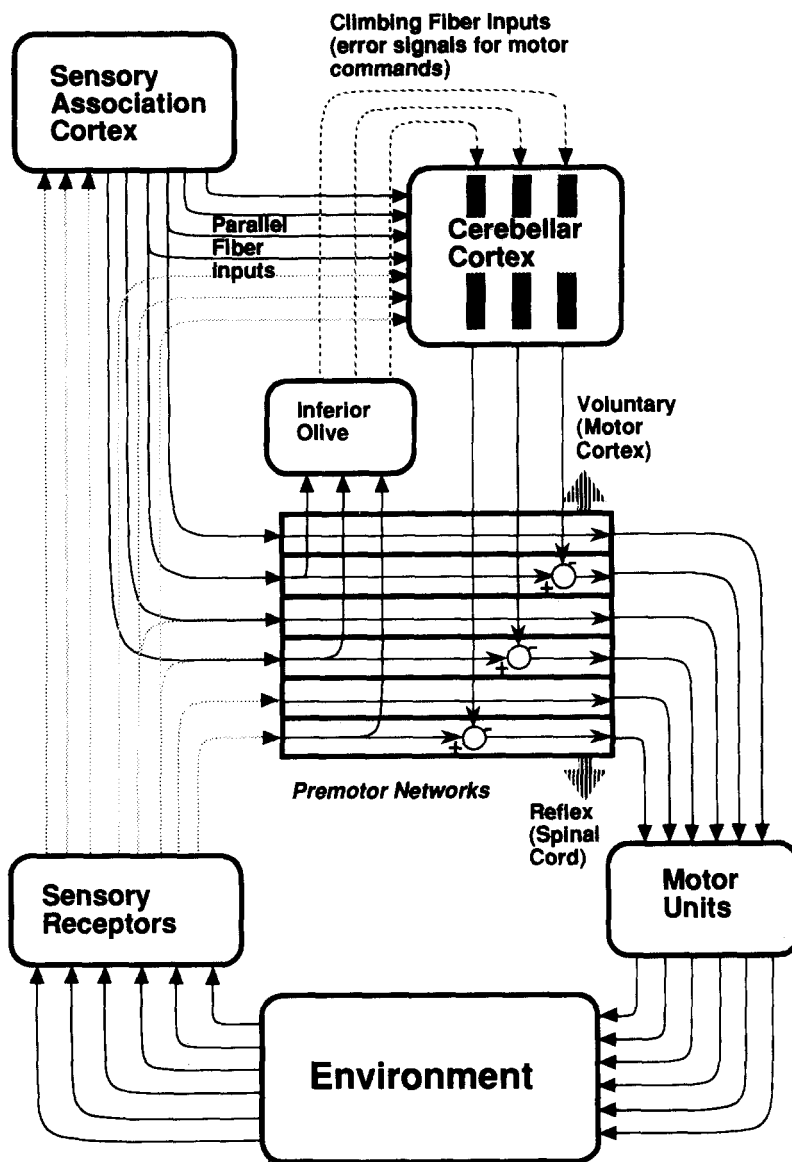


**Fig. 4.** A schematic diagram showing how cerebellar motor learning might be incorporated in sensory-motor control. Premotor networks are motor control networks that are located upstream of the motor neurons, and range in complexity from simple spinal reflexes (bottom of large rectangle) to motor cortical circuits controlling voluntary movement (top of large rectangle). Thus the top rectangle is assumed to contain the motor cortex. Some of the premotor networks are under the inhibitory influences of the cerebellar cortex. Parallel fibers to Purkinje cells carry vast amounts of information, both from the sensory receptors and from the cerebellum, which is necessary for coordinative and predictive control. Some of the parallel fibers represent desired motor pattern information and some represent current state information of the motor apparatus regardless of whether they originate from the sensory association cortex (solid curves) or from the sensory receptors (dotted line curves). The climbing fiber input is assumed to carry motor error signals represented in motor-command coordinates. This is realized by the closed-loop and one-to-one anatomical correspondence between each premotor network, the small region in the inferior olive and the microzone of the cerebellar cortex (shaded regions).

combination of motor units, the environment and sensory receptors in Fig. 4 correspond to feedback controller, inverse model, error and the controlled object in Fig. 2C, respectively. Parallel fiber inputs are assumed to carry the desired motor pattern information, in addition to the current states of the motor apparatus. We assume that climbing fiber responses represent motor commands generated by some of the premotor networks, i.e. networks that

are upstream of the motor neurons that include feedback controllers at the levels of the spine, the brain stem and the cerebral cortex (including the motor cortex). We do not necessarily assume that every premotor network literally compares a 'desired trajectory' with an 'actual trajectory'. It is, however, required that the premotor network calculate the motor error in the motor-command coordinates, which vanishes when the resultant movement is desirable. Based on the LTD in Purkinje cells, each longitudinal microzone in the cerebellar cortex, of 200  $\mu\text{m}$  in width and more than 50 mm in length, in conjunction with a small portion of the deep cerebellar nucleus that is connected to the microzone<sup>32,33</sup>, learns to execute predictive and coordinative control of different types of movements. This is realized by a closed-loop and one-to-one anatomical correspondence between each premotor network, a small region in the inferior olive, and a microzone of the cerebellar cortex<sup>32,33</sup>. If one premotor network is regulated by one microzone of the cerebellar cortex, then the latter must receive climbing fiber inputs from the specific part of the inferior olive that receives inputs from the earlier part of the same premotor network. With this anatomical organization, the cerebellar microzone is trained by the feedback error that represents the copy of the motor-error command generated by the corresponding premotor network. Ultimately, each microzone acquires an inverse model of a specific controlled object, and complements the relatively crude feedback control provided by the premotor networks. Thus, the activity of the corresponding earlier part of the premotor network decreases as cerebellar learning proceeds. However, the later part of the premotor circuit is quite active. Moreover, it must be noted that other premotor networks which are not connected to the cerebellum (see Fig. 4 for such independent premotor networks) may be active even after learning.

However, despite the crude nature of the signals from the premotor feedback networks, the premotor commands are the only source of motor coordinate information for training the cerebellum. There are two reasons why the relatively crude premotor command can serve as training information for the correct cerebellar command. First, the premotor command is not the teaching signal, but is instead the error signal. Second, although the premotor command is faulty, it, at least roughly, indicates the directions and magnitudes of cerebellar command modification. This latter point is actually controversial, since the range of firing frequencies of the climbing fibers is unusually low, and, hence, it has seemed difficult to understand how climbing fiber activity could convey directional or amplitude information. Rather, their apparent all-or-nothing firing characteristics may be useful for detection of somatic events<sup>49</sup>, providing information to the Purkinje cells about the occurrence of undesirable movements (penalty signal)<sup>43,46</sup>. However, because the LTD has a time constant of about one hour, even a low firing frequency can be integrated to give analog information. If the firing frequency is lower than the spontaneous level, it can give direction (negative) information. In the feedback-error-learning framework, the climbing fibers must be able to convey amplitude as well as directional information regarding the error. This prerequisite is supported in the

vestibulo-cerebellum<sup>31</sup>, but the problem is still unresolved for other regions. Based on an experimental design by Wang, Kim and Ebner<sup>50</sup>, we proposed a critical experimental test of our theory in which climbing fiber responses are measured in monkeys during a target change experiment in order to clarify this point<sup>48</sup>. By changing the direction and magnitude of the difference between the second target and the hand cursor presented on a video screen, our model predicts the direction and magnitude dependence of climbing fiber responses. Furthermore, such an experiment could be used to answer the basic question of whether movement errors are represented in sensory coordinates or in motor coordinates, by dissociating the trajectory error displayed on the video screen from the motor-command error. It could be accomplished, for example, by inverting one coordinate axis between the monkey's measured hand position and the displayed hand cursor position. Our theory requires that the climbing fiber responses be represented in motor coordinates (muscle activations) rather than in video screen coordinates.

### Concluding remarks

Computational models have not completely solved the puzzle of how and where cerebellar motor learning is conducted. These models have, however, introduced the notions of heterosynaptic plasticity for motor learning, acquisition of internal neural models of the motor apparatus, and necessary transformation of the error signals from the trajectory space to the motor-command space. With these concepts, neurophysiologists now have a framework on which to explore further the hardware responsible for the cerebellar motor learning.

### Selected references

- 1 Saltzman, E. L. (1979) *J. Math. Psych.* 20, 91–163
- 2 Hollerbach, J. M. (1982) *Trends Neurosci.* 5, 189–192
- 3 Kawato, M. (1992) *Attention and Performance XIV* (Meyer, D. and Kornblum, S., eds), pp. 821–849, MIT Press
- 4 Gilbert, P. F. C. and Thach, W. C. (1977) *Brain Res.* 128, 309–328
- 5 McCormick, D. A. and Thompson, R. F. (1984) *Science* 223, 296–299
- 6 Holmes, G. (1939) *Brain* 62, 1–30
- 7 Ito, M. (1970) *Int. J. Neurol.* 7, 162–176
- 8 Albus, J. S. (1975) *Trans. ASME J. Dyn. Syst. Meas. Cont.* 97, 220–227
- 9 Kawato, M., Furukawa, K. and Suzuki, R. (1987) *Biol. Cybern.* 57, 169–185
- 10 Atkeson, C. G. (1989) *Annu. Rev. Neurosci.* 12, 157–183
- 11 Barto, A. G. (1990) in *Neural Networks for Control* (Miller, T., Sutton, R. and Werbos, P., eds), pp. 5–58, MIT Press
- 12 Widrow, B. and Hoff, M. E. (1960) *1960 WESCON Conv. Rec.* IV, 96–104
- 13 Rumelhart, D. E. and McClelland, J. L. (1986) in *Parallel Distributed Processing*, p. 53, pp. 291–292, Bradford Books
- 14 Kuperstein, M. (1988) *Science* 239, 1308–1311
- 15 Jordan, M. I. (1990) *Attention and Performance XIII* (Jeannerod, M., ed.), pp. 796–836, Erlbaum
- 16 Jordan, M. I. and Rumelhart, D. E. (1992) *Cognit. Sci.* 16, 307–354
- 17 Rumelhart, D. E., Hinton, G. E. and Williams, R. J. (1986) *Nature* 323, 533–536
- 18 Mitchison, G. (1989) in *The Computing Neuron* (Durbin, R. C., Miall, R. C. and Mitchison, G., eds), pp. 35–53, Addison-Wesley
- 19 Kawato, M. (1990) in *Neural Networks for Control* (Miller, T., Sutton, R. and Werbos, P., eds), pp. 197–228, MIT Press
- 20 Katayama, M. and Kawato, M. (1991) in *Advances in Neural Information Processing Systems 3* (Lippmann, R. P., Moody,

### Acknowledgements

We thank Dr Swanson and the reviewers for their useful comments and suggestions. We thank A. G. Barto, J. C. Houk, M. Ito, R. C. Miall, S. Nagao and T. J. Sejnowski for their comments on an earlier version of the manuscript. We are grateful to E. Saltzman for his editing of the first draft of this paper. Supported by Human Frontier Science Project Research Grants. Preparation of the manuscript was done while we were in ATR Auditory and Visual Perception Research Laboratories, Japan.



- J. E. and Touretzky, D. S., eds), pp. 436–442, Morgan Kaufmann
- 21 Ito, M. and Nagao, S. (1991) *Comp. Biochem. Physiol.* 98C, 221–228
- 22 Marr, D. (1969) *J. Physiol.* 202, 437–470
- 23 Albus, J. S. (1971) *Math. Biosci.* 10, 25–61
- 24 Ito, M. (1989) *Annu. Rev. Neurosci.* 12, 85–102
- 25 Shibuki, K. and Okada, D. (1991) *Nature* 349, 326–328
- 26 Linden, D. J., Dickinson, M. H., Smeyne, M. and Connor, J. A. (1991) *Neuron* 7, 81–89
- 27 Crepel, F. and Jaillard, D. (1991) *J. Physiol.* 432, 123–141
- 28 Hirano, T. (1991) *Synapse* 7, 321–323
- 29 Fujita, M. (1982) *Biol. Cybern.* 45, 195–206
- 30 Maekawa, K. and Simpson, J. I. (1973) *J. Neurophysiol.* 36, 649–666
- 31 Simpson, J. I. and Alley, K. E. (1974) *Brain Res.* 82, 302–308
- 32 Oscarsson, O. (1980) in *The Inferior Olivary Nucleus. Anatomy and Physiology* (Courvillee, J., Montigny, C. D. and Lamarre, Y., eds), pp. 279–289, Raven Press
- 33 Ito, M. (1984) *The Cerebellum and Neural Control*, Raven Press
- 34 Stone, L. S. and Lisberger, S. G. (1990) *J. Neurophysiol.* 63, 1241–1261
- 35 Nagao, S. (1991) *Neurosci. Res.* 12, 169–184
- 36 Nagao, S. (1988) *Exp. Brain Res.* 73, 489–497
- 37 Gomi, H. and Kawato, M. *Biol. Cybern.* (in press)
- 38 Lisberger, S. G. (1988) *Science* 242, 728–735
- 39 Watanabe, E. (1985) *Neurosci. Res.* 3, 20–38
- 40 Gerrits, N. M. and Voogd, J. (1989) in *The Olivocerebellar System in Motor Control. Experimental Brain Research Series 17* (Strata, P., ed.), pp. 26–29, Springer-Verlag
- 41 Nagao, S. (1992) *NeuroReport* 3, 13–16
- 42 Sejnowski, T. L. and Lisberger, S. G. (1991) *Soc. Neurosci. Abstr.* 17, 1382
- 43 Houk, J. C. and Barto, A. G. in *Tutorial in Motor Behavior II* (Stelmach, G. E. and Requin, J., eds), pp. 71–100, Elsevier
- 44 Tsukahara, N., Bando, T., Murakami, F. and Oda, Y. (1983) *Brain Res.* 274, 249–259
- 45 Massone, L. and Bizzi, E. (1989) *Biol. Cybern.* 61, 417–425
- 46 Barto, A. G., Sutton, R. S. and Brouwer, P. S. (1981) *Biol. Cybern.* 40, 201–211
- 47 Miall, R. C., Weir, D. J., Wolpert, D. M. and Stein, J. F. *J. Motor Behav.* (in press)
- 48 Kawato, M. and Gomi, H. *Biol. Cybern.* (in press)
- 49 Gellman, R., Gibson, A. R. and Houk, J. C. (1985) *J. Neurophysiol.* 54, 40–60
- 50 Wang, J., Kim, J. H. and Ebner, T. J. (1987) *Brain Res.* 410, 323–329

## Rallpacks: a set of benchmarks for neuronal simulators

Upinder S. Bhalla, David H. Bilitch and James M. Bower

*The field of computational neurobiology has advanced to the point where there are several general-purpose simulators to choose from. These cater to various niches in the world of realistic neuronal models, which range from the molecular level to descriptions of entire sensory modalities. In addition, there are numerous custom-designed simulations, adaptations of electrical circuit simulators, and other specific implementations of neurobiological models. As a first step towards evaluating this disparate set of simulators and simulations, and towards establishing standards for comparisons of speed and accuracy, we describe a set of benchmarks. These have been given the name 'Rallpacks' in honor of Wilfrid Rall, who pioneered the study of neuronal systems through analytical and numerical techniques.*

Numerical methods for computing the properties of neuronal models have existed at least since the 19th century, when Lord Kelvin first studied the equations describing signal propagation for the first undersea cables. This problem is mathematically identical to the description of the passive properties of cellular membranes, and the 'cable equations' underlie all realistic neuronal models. The description of the active properties of membranes by Hodgkin and Huxley<sup>1</sup> in the 1950s was the second major conceptual advance in the field. Even the most sophisticated simulations carried out today are essentially implementations, in greater and greater detail, of the formulation of neurons in terms of these passive and active properties. The application of these equations to neuronal systems has been undertaken from the 1950s onward, notably by Wilfrid Rall<sup>2</sup>.

### Levels of description

Neuronal systems have features of interest and functional significance at all the levels of detail that have been studied<sup>3</sup>, from the molecular to the

systems level. An especially keenly studied section of this field has been at the level of the single neuron, which has consequently seen a proliferation of simulations and simulators<sup>4,5</sup>. The present set of 'Rallpacks' are intended to provide a standard for evaluating the basic numerical capabilities of this disparate variety of simulators at the single neuron level, and to provide a degree of confidence in the reproducibility of simulations carried out on them.

### What simulators do

As alluded to above, realistic single neuron simulators must at least solve the equations describing the passive and active properties of neurons. A brief overview of this process follows.

*Passive properties.* The passive cable equations are partial differential equations, and may be expressed as:

$$\lambda^2 \left( \frac{\partial^2 V}{\partial x^2} \right) - V - \tau \left( \frac{\partial V}{\partial t} \right) = 0$$

where  $\lambda$  is the cable length constant and  $\tau$  is the time constant.

Several methods may be employed in solving these equations<sup>6</sup>, including Laplace transforms and discretization in space and time. The latter is the method of choice for almost all neuronal simulators. Briefly, it may be thought of as a process of subdividing the description of the model in space and in time, so that values calculated for discrete positions and times may be used to approximate the real, smoothly varying system. The process of spatial discretization is accomplished by dividing the neuronal model into compartments, which are simply short cylindrical lengths of cell membrane of uniform diameter and electrical properties. The problem is then reduced to a system of coupled ordinary differential equations

*Upinder S. Bhalla, David H. Bilitch and James M. Bower are at the Division of Biology, California Institute of Technology 216-76, Pasadena, CA 91125, USA.*